Natural Science Report, Ochanomizu University, Vol. 15, No. 2, 1964
お茶の水女子大学 自然科学報告 第15巻 第2号

Convective Motion of Fluid Mass Due to an Instantaneous Point Source of Heat

Yuko Oshima (大島裕子)

Department of Physics, Faculty of Science
Ochanomizu University, Tokyo

(*Received September 10, 1964*)

I. Introduction

One of the most spectacular scene ever we had seen may be a rising fire ball and mushroom cloud caused by an atomic explosion. We have seen in many photographs and movies that an air mass heated by the energy released from the nuclear reaction rises quickly and forms a tremendous volume of mushroom cloud and slowly diffuses away. The purpose of this work is to investigate the physical background of this kind of phenomena, that is, to study the free convection flow caused by an instantaneous point source of heat in a uniform medium. Of course, this is one of the most important problem in industry and meteorology also.

The flow fields caused by thermal buoyancy effect have been studied over centuries and the basic equations governing them and the solutions for various typical cases have been described in numerous text books[1)2)3)]. The early investigations were concerned mainly with steady free convection from a heated body with simple shape, e. g., a point source, a flat plate and a circular cylinder etc. and tried to find out similar solutions using the boundary layer approximation. On the other hand, investigators of meteorology have been interested in the unsteady convective motion of air masses in connection with the developments of cumulus clouds. A great number of reports of observations and calculations have been published on the subject. Among these, the following are noteworthy concerning the present study. Woodward carried out observations riding on a glider in 'thermals' (buoyant air masses) in the atmosphere and investigated the nature of vertical motions of air[4)]. Scorer derived formulae for the width of the thermals and the distance travelled by them on the dimensional analysis, and he made experiments in which the buoyant air mass was simulated by a liquid mass colored with dye and falling in water at rest[5)]. Morton, Taylor and Turner presented the theories of convection from maintained and instantaneous sources[6)]. They

treated a buoyant mass as a whole instead of investigating its internal structure, and discussed the final height of bouynat mass as function of buoyancy and density gradient. They carried out laboratory experiments by releasing a light fluid in a tank filled with heavier fluid, and observed the motion of smokes and cloud and in the atmosphere compared with their predictions. Further, Turner investigated the convective motion of buoyant liquid comparing with that of vortex rings and vortex pairs[7)8)]. Morton calculated the flow and the temperature field in a thermal vortex ring and in the ambient fluid[9)]. His analysis is carried out by expanding in series in Rayleigh number A and restricted in the case of small A, so that the results are not applicable for many real phenomena.

The unsteady free convective flows are so complicated in nature that the exact and detailed analysis of them is very difficult and would have to resort to very extensive numerical calculations. However, there is the possibility for the similarity solution (self-similar solution) in the case of free convection due to a point source of heat[10)]. Moreover in the early stage of buoyant motion, the fluid velocities are so small that linearized approximation is allowable. By the use of this procedure, a great deal of informations about these phenomena may be supplied : e. g., How the distance travelled by a buoyant mass of liquid is affected by Rayleigh number (or Grashof number) and Prandtl number? etc. The process of this approximation is described in section II and calculation for a special case is shown. This result seems to be in good agreement with the experimental results presented in section III. General characteristics of the velocity and temperature field will be analysed by this method and reported in future.

As mentioned above, the laboratory experiments concerning the unsteady free convection have carried on by releasing a mass of a light (or heavy) fluid into a heavier (or lighter) medium at rest and by observing only the height and growth of scale of the 'buoyant' mass. The measurements of the transient temperature of the fluid in such cases need rather delicate techniques. The optical interferometry is most favorable for this purpose, because it has very high sensitivity to small temperature change and it does not disturb the field, but the ordinary Mach-Zehnder interferometer is so hard to adjust that it is almost unpractical for actual measurements of temperature field in the fluid. Then we have developed a double refraction interferometer[11)], which is very easy to adjust yet keeps all the merits of the Mach-Zehnder interferometry.

The flow patterns were visualized by introducing small aluminum powders on the field. The media in use are water and the mixture of water and glycerin. By varing the heat quantity released from a

source, the temperature of water, and the mixing ratio of water and glycerin, the experiments for the fairy wide range of Grashof number and Prandtl number were performed. The details of conditions and results of experiments are presented in section III and some discussions are made.

II. Analysis of Convective Motion

Basic Equation

Let us consider the flow and temperature field caused by an instantaneously released heat energy at a point in a uniform medium. The temperature field immediately after the time of heat supply is illustrated in Fig. 1 (a). As the time passes, the mass of the heated fluid slowly moves upward due to buoyancy force being resisted by viscous effect, the heat diffuses into the ambient fluid, and the resulting temperature distribution is as shown in (b). The flow caused by this convective motion deforms the temperature distribution, and finally the buoyant fluid mass forms the mushroom shape as shown in (c).

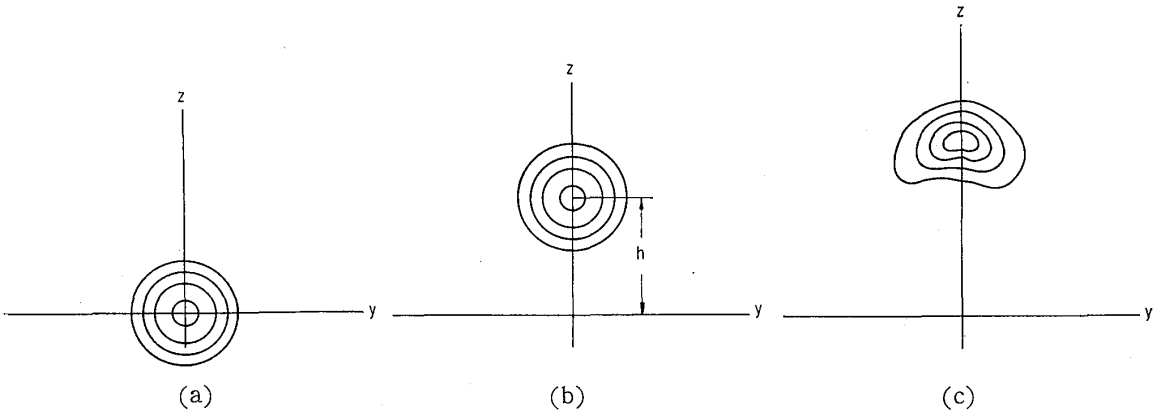

Fig. 1 (a), (b), (c). Isothermals in a buoyant mass of liquid.

The basic equation which we should consider for this problem are the equations of conservation of mass, momentum and energy. For an incompressible fluid flow, they are

$$\begin{aligned} &\operatorname{div} \boldsymbol{v}=0\,, \\ &\frac{\partial \boldsymbol{v}}{\partial t}+(\boldsymbol{v}\cdot\operatorname{grad})\boldsymbol{v}=\boldsymbol{B}\theta-\frac{1}{\rho}\operatorname{grad} p+\nu\nabla^2\boldsymbol{v}\,, \\ &\frac{\partial \theta}{\partial t}+(\boldsymbol{v}\cdot\operatorname{grad})\theta=\kappa\nabla^2\theta\,, \end{aligned} \tag{1}$$

respectively, where $\boldsymbol{v}$ is the velocity of the fluid, p is the pressure, θ is the increase in temperature over that of the undisturbed value, and t is the time, ρ, ν and κ are the density, the kinematic viscosity and the thermal diffusivity of the fluid, respectively. The thermal

buoyancy factor $\boldsymbol{B}$ is the product of the thermal expansion coefficient β, and the acceleration of gravity $\boldsymbol{g}$, i.e. $\boldsymbol{B}=-\beta\boldsymbol{g}$. The temperature difference θ is assumed so small in the whole field that these physical properties of the fluid may be supposed to be independent of temperature change. Since the velocity of convective flow is also small, the viscous dissipation term in the energy equation has been neglected.

We adopt a rectangular co-ordinates, the x- and the y-axes being in a horizontal plane, the z-axis along the direction of the buoyancy force. In this co-ordinate system, the basic equations are

$$\begin{aligned}
&\frac{\partial u}{\partial x}+\frac{\partial v}{\partial y}+\frac{\partial w}{\partial z}=0,\\
&\frac{\partial u}{\partial t}+u\frac{\partial u}{\partial x}+v\frac{\partial u}{\partial y}+w\frac{\partial u}{\partial z}=-\frac{1}{\rho}\frac{\partial p}{\partial x}+\nu\left(\frac{\partial^2 u}{\partial x^2}+\frac{\partial^2 u}{\partial y^2}+\frac{\partial^2 u}{\partial z^2}\right),\\
&\frac{\partial v}{\partial t}+u\frac{\partial v}{\partial x}+v\frac{\partial v}{\partial y}+w\frac{\partial v}{\partial z}=-\frac{1}{\rho}\frac{\partial p}{\partial y}+\nu\left(\frac{\partial^2 v}{\partial x^2}+\frac{\partial^2 v}{\partial y^2}+\frac{\partial^2 v}{\partial z^2}\right),\\
&\frac{\partial w}{\partial t}+u\frac{\partial w}{\partial x}+v\frac{\partial w}{\partial y}+w\frac{\partial w}{\partial z}=B\theta-\frac{1}{\rho}\frac{\partial p}{\partial z}+\nu\left(\frac{\partial^2 w}{\partial x^2}+\frac{\partial^2 w}{\partial y^2}+\frac{\partial^2 w}{\partial z^2}\right),\\
&\frac{\partial \theta}{\partial t}+u\frac{\partial \theta}{\partial x}+v\frac{\partial \theta}{\partial y}+w\frac{\partial \theta}{\partial z}=\kappa\left(\frac{\partial^2 \theta}{\partial x^2}+\frac{\partial^2 \theta}{\partial y^2}+\frac{\partial^2 \theta}{\partial z^2}\right),
\end{aligned}\tag{2}$$

where u, v and w are the components of fluid velocity. Let us consider that a definite amount of heat is released instantaneously at the origin of the co-ordinate system at $t=0$. The initial conditions are

$$u=v=w=\theta=0 \quad \text{at} \quad t=0,$$

except at the origin, where there are singularities in velocity and temperature. For $t>0$, the whole field is regular, and the boundary conditions are

$$u=v=w=\theta=0 \qquad \text{at infinity,} \tag{3}$$

Further we may assume the motion and temperature distribution to be symmetrical about the z-axis, then

and

$$\left.\begin{aligned}
&u=v=0,\\
&\frac{\partial w}{\partial x}=\frac{\partial w}{\partial y}=0,\\
&\frac{\partial \theta}{\partial x}=\frac{\partial \theta}{\partial y}=0,
\end{aligned}\right\} \quad \text{at } x=y=0. \tag{4}$$

Since the heat dissipation is neglected, the excess of the heat quantity in the whole field over the undisturbed state remains constant:

$$Q=\rho c_V\int_{-\infty}^{\infty}\!\!\int\!\!\int \theta\, dx\, dy\, dz,$$

where c_V is the specific heat of the fluid at constant volume, or

$$\iiint_{-\infty}^{\infty} \theta \, dx\, dy\, dz = \text{const.} = \frac{Q}{\rho c_V} = Q' . \tag{5}$$

Self-similarity

The parameters which concern the present problem are thermal diffusivity κ, the kinematic viscosity ν, the thermal buoyancy factor B and the total amount of temperature excess Q', as easily seen from the above discussions. The dimensions of these quatities are

$$[\kappa]=[L^2T^{-1}],$$
$$[\nu]=[L^2T^{-1}],$$
$$[B]=[LT^{-2}C^{-1}],$$
$$[Q']=[L^3C],$$

where $[L]$, $[T]$ and $[C]$ denote the dimensions of length, time and temperature, respectively. Because $[\nu]=[\kappa]$ and $[BQ']=[\nu^2]$, we can define the two non-dimensional parameters as follows:

$$\sigma=\nu/\kappa ,$$
$$G=\frac{BQ}{\rho c_V \nu^2} . \tag{6}$$

Usually σ is called the Prandtl number, and G is a parameter which corresponds to the Grashof number in the case of natural convection from a heated body. All the flow quantities are determined by r, t and these four parameters. Then, we see by the dimensional consideration, that all the non-dimensionalized quantities in the flow field are determined by σ, G and only one other parameter. It has a form r/t^{δ}, where r is a spatial co-ordinate and δ is a certain constant which shall be determined by physical considerations or experimental evidence. This is the self-similarity.*

Experimentally it is shown that the height of the highest temperature point from the origin is always proportional to $\sqrt{t}$, then we introduce a characteristic length $h=2\sqrt{\kappa t}$. Using this characteristic length each variable is non-dimensionalized, respectively as follows:

$$x=hX, \quad y=hY, \quad z=hZ,$$
$$u=\frac{2\kappa}{h}U, \quad v=\frac{2\kappa}{h}V, \quad w=\frac{2\kappa}{h}W, \tag{7}$$
$$\theta=\frac{Q}{\rho c_V}\frac{\Theta}{h^3} .$$

* On the contrary, the free convective flow caused by line source of heat streched horizontally is not self-similar, because a characteristic for this case is the temperature excess per unit width and it has the dimension $[L^2C]$.

In the present study we treat the free convective motion in an unlimitted fluid without any boundary surfaces, then the variation of the pressure may be neglected and terms expressing its gradient are omitted hereafter.

In terms of these non-dimensional quantities the basic equations are transformed into the following forms:

$$\frac{\partial V}{\partial X}+\frac{\partial V}{\partial Y}+\frac{\partial W}{\partial Z}=0\,,$$

$$(U-X)\frac{\partial U}{\partial X}+(V-Y)\frac{\partial U}{\partial Y}+(W-Z)\frac{\partial U}{\partial Z}-U=\frac{\sigma}{2}\nabla^2 U\,,$$

$$(U-X)\frac{\partial V}{\partial X}+(V-Y)\frac{\partial V}{\partial Y}+(W-Z)\frac{\partial V}{\partial Z}-V=\frac{\sigma}{2}\nabla^2 V\,, \tag{8}$$

$$(U-X)\frac{\partial W}{\partial X}+(V-Y)\frac{\partial W}{\partial Y}+(W-Z)\frac{\partial W}{\partial Z}-W=\frac{\sigma}{2}\nabla^2 W+\frac{G}{4}\Theta\,,$$

$$(U-X)\frac{\partial \Theta}{\partial X}+(V-Y)\frac{\partial \Theta}{\partial Y}+(W-Z)\frac{\partial \Theta}{\partial Z}-3\Theta=\nabla^2\Theta\,.$$

The boundary conditions given by eqs. (3)~(5) are easily rewritten in terms of new variables, especially the last equation is expressed as

$$\int_{-\infty}^{\infty}\!\!\int\!\!\int \Theta\, dX\, dY\, dZ=1\,. \tag{9}$$

The development of the general features of the field as shown in Fig. 1 suggests that it may be convenient to translate the origin of the co-ordinate system as the buoyant mass rises along the vertical axis. Then we put

$$Z'=Z-Z_0\,,$$

and accordingly $W'=W-Z_0$.

In the frame of this translated co-ordinate system, the phenomena are always axisymmetric and moreover are nearly spherically symmetric at least in the stage of beginning of the convection. Therefore it is natural to use the spherical polar co-ordinate, that is, to transform (X, Y, Z') and (U, V, W') into (R, ϑ, φ) and $(V_R, V_\vartheta, V_\varphi)$ respectively. Remembering that the velocity and the temperature fields are axisymmetric that is

$$\frac{\partial}{\partial \varphi}\equiv 0\,, \qquad V_\varphi=0\,,$$

we obtain the following equations:

$$\frac{\partial V}{\partial R}+\frac{2}{R}V_R+\frac{1}{R}\frac{\partial V_R}{\partial \vartheta}+\frac{\cot\vartheta}{R}V_\vartheta=0\,,$$

$$(V_R-R)\frac{\partial V_R}{\partial R}+\frac{V_\vartheta}{R}\frac{\partial V_R}{\partial \vartheta}-\frac{V_\vartheta^2}{R}-V_R-Z_0\cos\vartheta$$
$$=\frac{2}{\sigma}\left(\frac{\partial^2 V_R}{\partial R^2}+\frac{2}{R}\frac{\partial V_R}{\partial R}+\frac{1}{R^2}\frac{\partial^2 V_R}{\partial \vartheta^2}+\frac{\cot\vartheta}{R}\frac{\partial V_R}{\partial \vartheta}\right.$$
$$\left.-\frac{2}{R^2}V_R-\frac{2}{R^2}\frac{\partial V_\vartheta}{\partial \vartheta}-\frac{2\cot\vartheta}{R^2}V_\vartheta\right)+\frac{G}{4}\Theta\cos\vartheta\,,$$

$$(V_R-R)\frac{\partial V_\vartheta}{\partial R}+\frac{V_\vartheta}{R}\frac{\partial V_\vartheta}{\partial \vartheta}+\frac{V_R V_\vartheta}{R}-V_\vartheta+Z_0\sin\theta \tag{11}$$
$$=\frac{\sigma}{2}\left(\frac{\partial^2 V_\vartheta}{\partial R^2}+\frac{2}{R}\frac{\partial V_\vartheta}{\partial R}+\frac{1}{R^2}\frac{\partial^2 V_\vartheta}{\partial \vartheta^2}+\frac{\cot\vartheta}{R^2}\frac{\partial V_\vartheta}{\partial \vartheta}\right.$$
$$\left.+\frac{2}{R^2}\frac{\partial V_R}{\partial \vartheta}-\frac{V_\vartheta}{R^2\sin^2\vartheta}\right)-\frac{G}{4}\Theta\sin\theta\,,$$

$$(V_R-R)\frac{\partial \Theta}{\partial R}+\frac{V_\vartheta}{R}\frac{\partial \Theta}{\partial \vartheta}-3\Theta$$
$$=\frac{1}{2}\left(\frac{\partial^2\Theta}{\partial R^2}+\frac{2}{R}\frac{\partial \Theta}{\partial R}+\frac{1}{R^2}\frac{\partial^2\Theta}{\partial \vartheta^2}+\frac{\cot\vartheta}{R^2}\frac{\partial \Theta}{\partial \vartheta}\right).$$

The boundary conditions are

$$\vartheta=0 \text{ and } \pi\,;\qquad V_\vartheta=0 \text{ and } \frac{\partial V_R}{\partial \vartheta}=0\,,$$
$$R\to\infty\,;\qquad V_R=-Z_0\cos\vartheta\,,\qquad V_\vartheta=Z_0\sin\vartheta\,, \tag{12}$$

and

$$2\pi\int_0^\infty\int_0^{2\pi}\Theta R^2\sin\vartheta\cdot dR\,d\vartheta=1\,. \tag{13}$$

These equations (11) and boundary conditions (12) and (13) determine the V_R, V_ϑ and Θ as functions of R and ϑ, which constitute the self-similar solution for this problem.

Approximate Solution for the Buoyant Motion

For the comparison with the experiments which are described in section III, we are interested in the distance travelled by the buoyant mass of the liquid and the temperature distribution in it in the early period of convection. Since the velocity of the fluid is very small as well as the temperature excess Θ, at this stage, the linearized approximation may be effectively used. The temperature excess is supposed to distribute symmetrically about the origin $R=0$, and we confine our considerations only about the states on the vertical axis ($\vartheta=0$ or π).

In this approximation we need only to treat the following equations

$$\frac{\partial^2 V_R}{\partial R^2}+2\left(\frac{1}{R}+\frac{R}{\sigma}\right)\frac{\partial V_R}{\partial R}+2\left(\frac{1}{\sigma}-\frac{1}{R^2}\right)V_R+\frac{2}{\sigma}Z_0=\frac{G}{2\sigma}\Theta\,,$$
$$\frac{1}{2}\frac{\partial^2\Theta}{\partial R^2}+\left(R+\frac{1}{R}\right)\frac{\partial\Theta}{\partial R}+3\Theta=0\,, \tag{14}$$

with the boundary conditions

$$R\to\infty\,;\qquad V_R=-Z_0\,,$$
$$4\pi\int_0^\infty \Theta R^2 dR=1\,, \tag{15}$$

in order to determine V_R and Θ as functions of R only.

From the second equation of (14) and (15), we have

$$\Theta=\frac{1}{\pi^{3/2}}e^{-R^2}\,. \tag{16}$$

This solution gives the temperature pattern as shown in Fig. 1 (b). The typical mushroom shape as shown in Fig. 1 (c) may result from the original equation. Therefore, in the present approximation the highest temperature in the flow field is observed at a point of $R=0$, its temperature is proportional to G and h^{-3}. In other words, the highest temperature is proportional to the energy supplied and $t^{-3/2}$.

The distance travelled by the buoyant mass of liquid Z_0 is the height of the point of the highest temperature above the point of heat release and it is determined by the equations (14) and (15) together with the velocity V_R. It is easily shown that Z_0 and V_R are proportional to G, and this prediction is to be compared with the experiments.

III. Experiments

Apparatus

A $18.6\times5.9\times20\ \mathrm{cm}^3$ fluid container was made from pyrex glass, and the two side walls of it, each of $18.6\times20\ \mathrm{cm}^2$, were finished optically flat and fixed completely paralell with each other. (Photo. 1.) At the inner bottom of it, two sets of electric terminals were atached for heating. Pure water or mixture of glycerin and water is filled in it keeping temperature and mixing ratio uniformly throughout the container.

The point source was made of a small tungsten coil of about 7 ohms placed 15 mm above the bottom. This coil was heated by an electric current in a short time, and its intensity and duration were precisely controlled by a control unit specially prepared. A photograph of this control system is shown in Photo. 2.

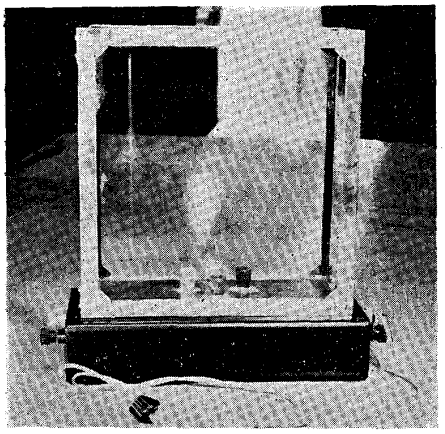

Photo. 1. Water tank.

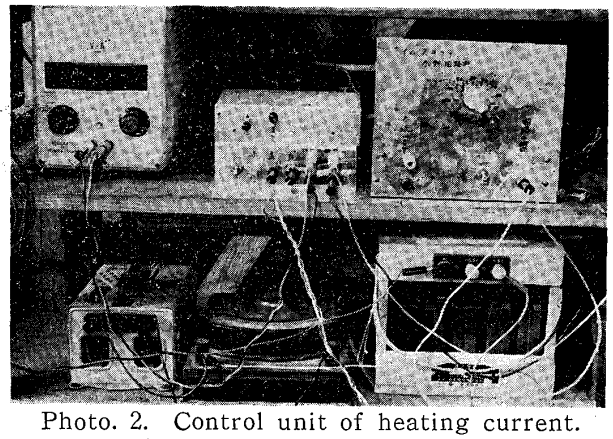

Photo. 2. Control unit of heating current.

For optical measurements, a double refraction interferometer, similar to the system developed by R. Chevalerias, Y. Laton and C. Veret (11) has been constructed. This apparatus is very easy to operate and yet has high sensitivity than the ordinary shlielen system. The diagram of this system is shown in Fig. 2. As seen in figure, two Wollaston prisms and crossed polarizer are used instead of knife edge of the ordinary shlieren system. These Wollaston prisms (compensators) have dimensions as shown in Fig. 3. Passing through the condenser lens C and the first polarizer P, the light beam from lamp house S focuses at the pin hole H and the first compensator Q_1. The compensator is in the focal plane of the spherical mirror M_1; working section bounded by the glass walls of good optical quality (water container T) is crossed by the paralell light. The spherical mirror M_2 makes the image of compensator Q_1 or that of the source S at the compensator Q_2. The mirror M_2 also makes the image of the working section in the plane of the observation screen E. An analyser A and the filter F are placed before the screen E. The difference in the optical path between the two interfering beams depends on the difference of the dencity, or that of the temperature of the fluids passed by the beams.

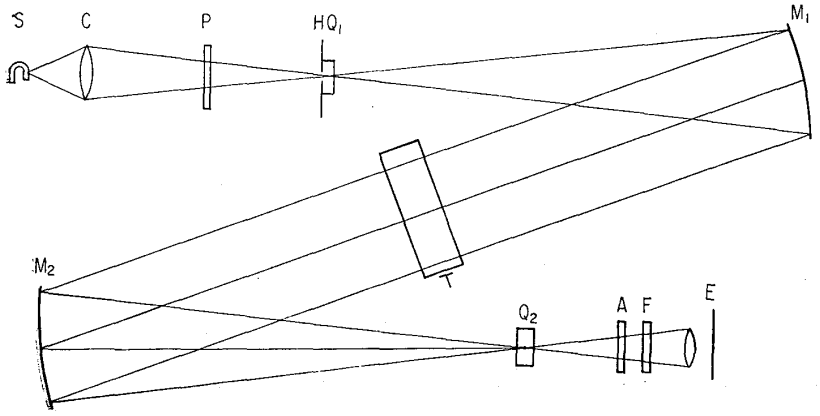

Fig. 2. Arrangement for a double refraction interferometry.

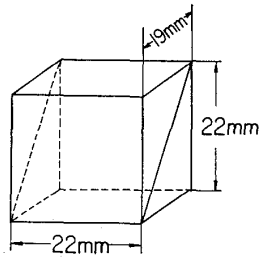

Fig. 3. Wollaston prism.

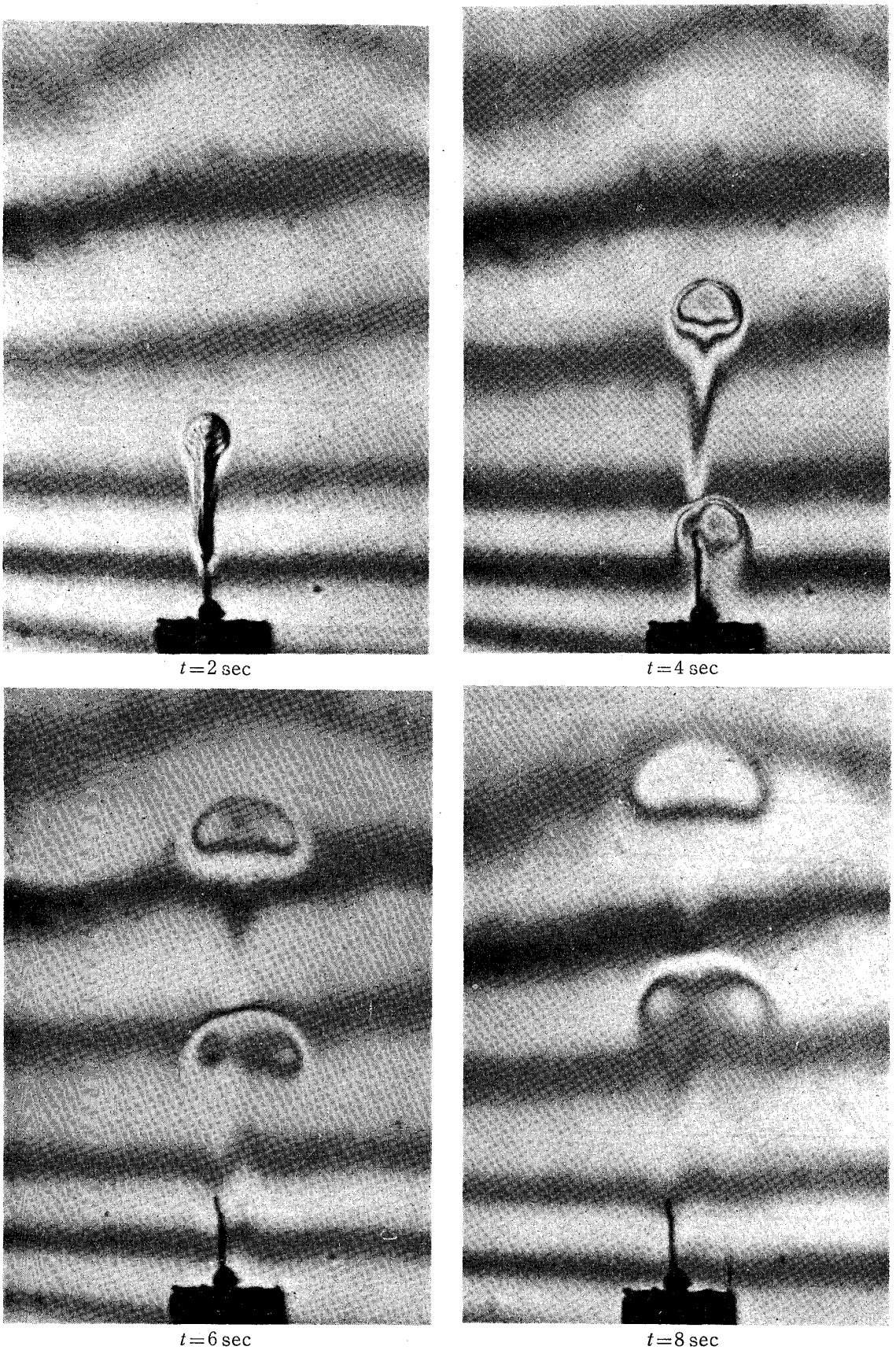

$t=2$ sec $t=4$ sec

$t=6$ sec $t=8$ sec

Photo. 3. Interferogram of temperature field, water, 25°C.

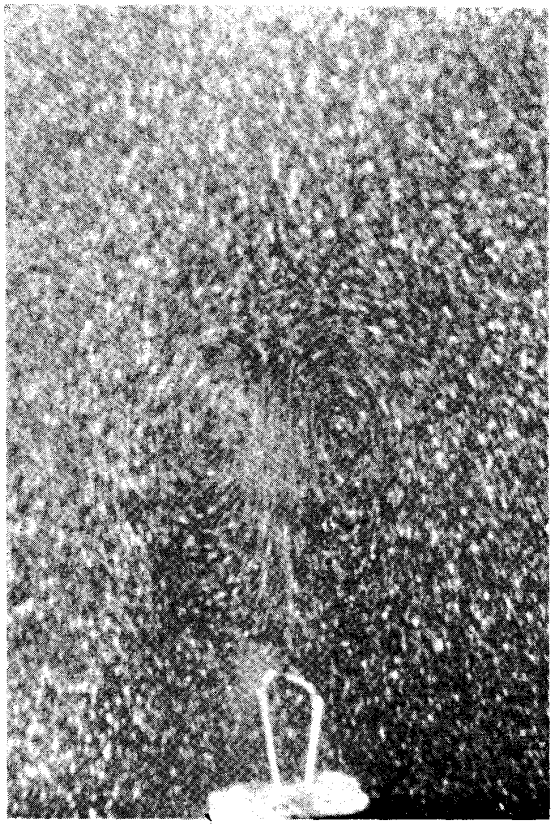

$t=2$ sec

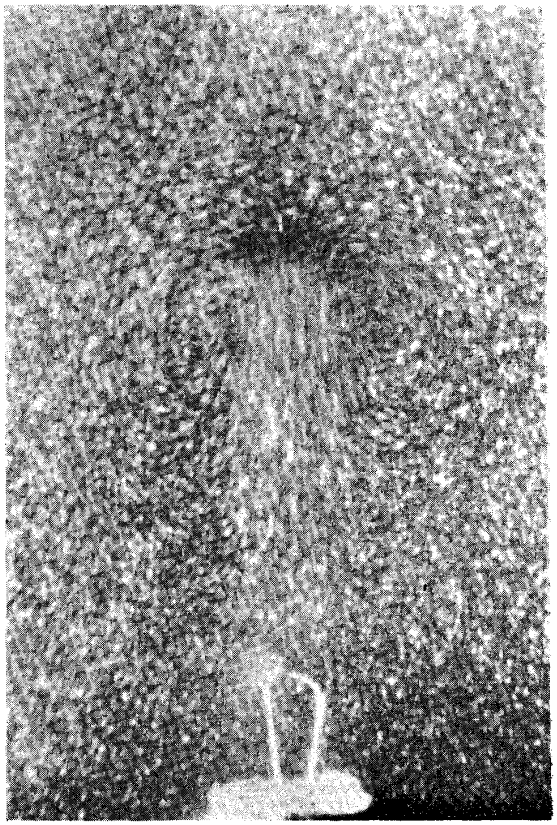

$t=4$ sec

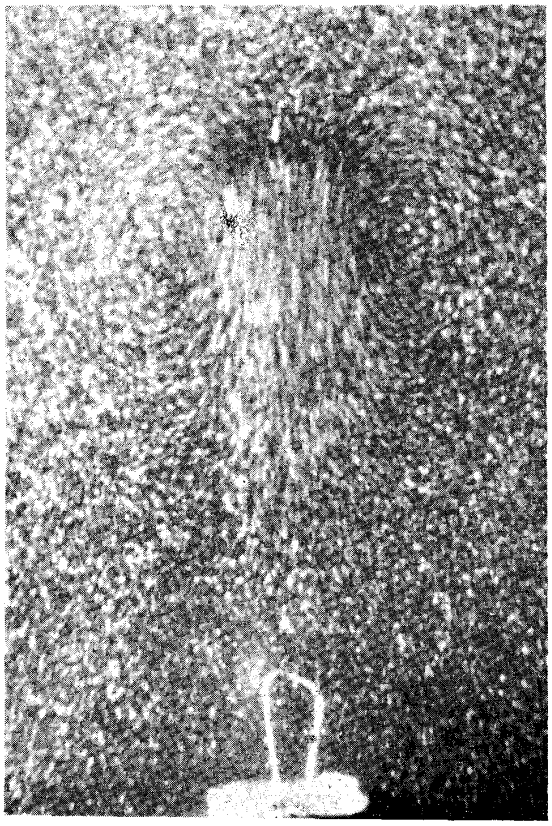

$t=6$ sec

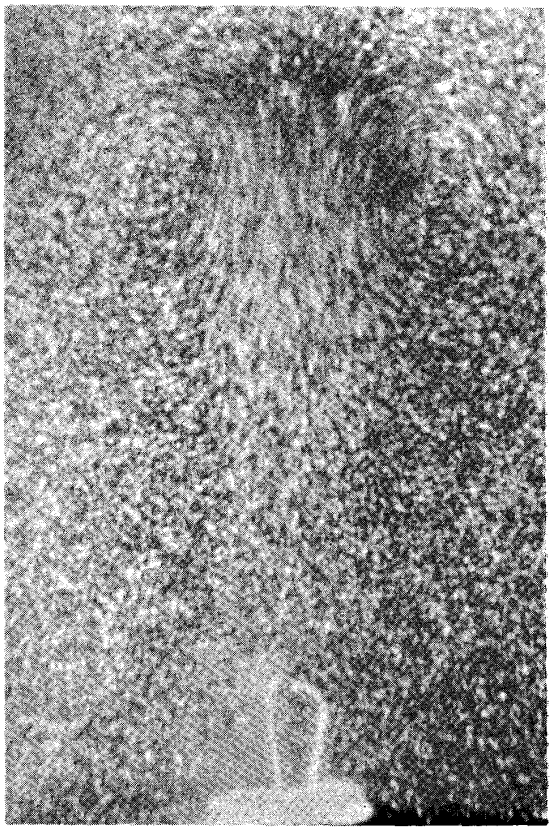

$t=8$ sec

Photo. 4. Flow pattern water, 25°C.

The interferograms were taken at intervals of two seconds after the heating of the source using a motor-driven camera system placed at the observation screen E. A typical example of a series of a photographs are shown in Photo. 3. As seen in photographs, the interferometer was adjusted so as to make a unifringe field of monochromatic light of 5461Å separated by the filter F from a light of mercury lamp, and then the fringe shifts correspond to the temperature difference. The position of the point of the highest temperature is easily determined from these photographs, moreover they give temperature distribution of the whole field qualitatively, though it needs rather tedious work in order to obtain quantitative results.

On the other hand, to visualize the flow field, we made use of the aluminum dust method, and took photographs in 1 sec exposure at the same condition as the interferometry. Some examples of a series of photographs under the same condition as Photo. 3 are shown in Photo. 4 for comparison. They clearly show the nature of the flow around a vortex ring.

Scope of Experiments

The experiments were carried out in pure water at various temperature and in the mixture of glycerin and water with various mixing ratios maintained at 20°C. The heating energy was changed from 0.14 cal to 0.28 cal by controlling the electric currents (280 mA and 350 mA), and the duration (1.04 sec and 1.30 sec) of it, but maximum energy is limitted by a bubble formation at the heat source. The values of the physical constants under various experimental conditions are tabulated in Table (a) and (b). It may be noted that the

Table (a)

Water

°C	ν $\times 10^{-2}$ $cm^2\ sec^{-1}$	κ $\times 10^{-3}$ $cm^2\ sec^{-1}$	β $\times 10^{-3}$	σ	G_1	G_2
5	1.519	1.36	0.040	11.16	24.3	30.8
10	1.308	1.37	0.087	9.55	71.3	89.2
15	1.141	1.38	0.150	8.31	161	201
20	1.007	1.40	0.200	7.20	276	345
25	0.897	1.42	0.250	6.34	435	546
30	0.804	1.45	0.302	5.53	660	823
35	0.720	1.47	0.350	5.00	933	1165
40	0.661	1.49	0.400	4.43	1290	1160
45	0.605	1.51	0.430	4.05	1652	2080
50	0.556	1.54	0.458	3.67	2090	2620
55	0.514	1.56	0.490	3.33	2640	3290

Table (b)

Mixture of glycerin and water

Content of glycerin %	ν $\times 10^{-2}$ cm^2 sec^{-1}	κ $\times 10^{-3}$ cm^2 sec^{-3}	β $\times 10^{-3}$	σ	G_1	G_2
10	1.280	1.364	0.23	9.39	413	472
20	1.687	1.305	0.26	12.91	252	317
30	2.230	1.260	0.29	17.76	166	208
40	3.410	1.207	0.32	28.28	81.0	101
50	5.380	1.159	0.35	46.3	36.8	45.9
60	9.480	1.111	0.38	85.4	13.3	16.6

value of coefficient of thermal expansion of water strongly depends on the temperature, in fact it is null at 3.96°C. On the other hand, the mixing ratio of glycerin and water seriously affects the value of kinematic viscosity.

Experimental Results.

Under the above-mentioned experimental conditions the parameters varies in the range $3<\sigma<85$ and $13<G<3290$, respectively. The height of the point of the highest temperature is proved to be proportional to the square roots of the time as shown in Fig. 4 (a), (b). In almost all cases, the points corresponding to the measurements in a series lie so fairly on a straight line respectively that the individual points are not shown but for a few examples. This relation has been used to reduce the self-similar equation. As seen in this figure, the gradients of straight lines increase with temperature at low temperatures, but over 25°C such a definite tendency is not found. This gradient increases evidently with the increase in the heating energy as shown in Fig. 5. In Fig. 6 (a), (b), these gradients or the non-dimentionalized heights of point of the highest temperature Z_0 are plotted against the Grashof number. As the linearized approximation theory predicts, the values of Z_0 are proved to be proportional to G for the same σ. The calculated result for the special case when $\sigma=1$, and $G=8\pi^{3/2}$ is also shown in the same figure which is in good accord with the experiment. Fig. 7 which shows the relation between Z_0/G and σ suggests that Z_0 is proportional to the Prandtl number also in the present case.

Acknowledgements

The auther would like to acknowledge the useful advice of Prof. S. Asaka who supervised this work, and also many thanks due to Dr. K. Oshima for his encouragement and discussions. This work has been partly supported by the grant-in-aid for the fundamental scientific research from the Ministry of Education.

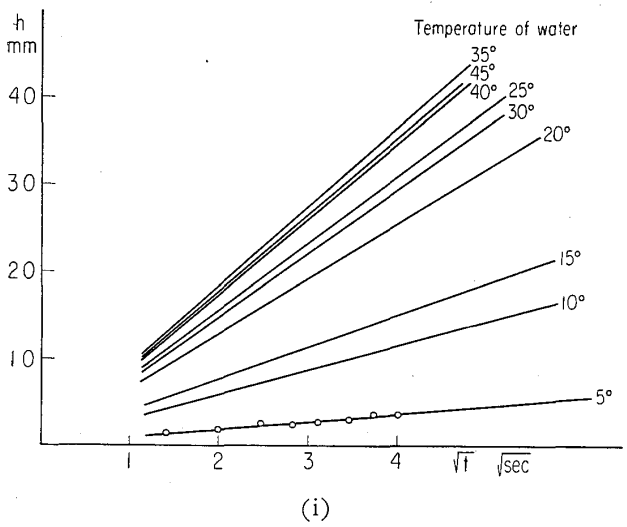

(i)

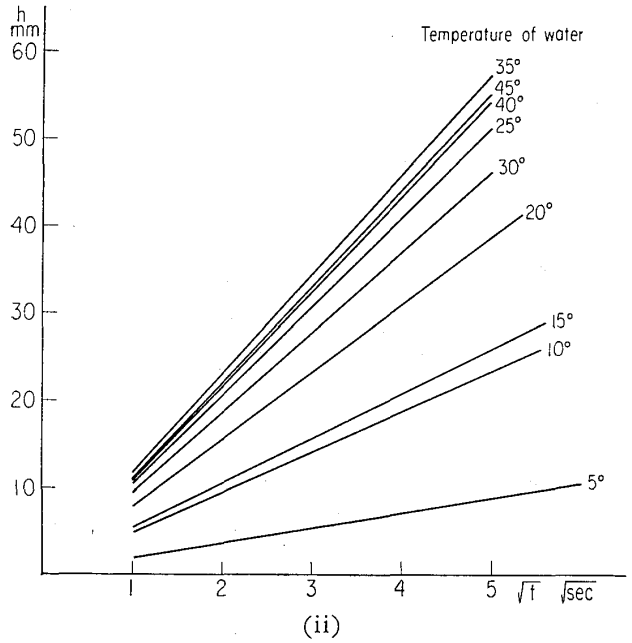

(ii)

Fig. 4 (a). $h \sim \sqrt{t}$ water (i). For various temperature of the water, heating current 280 mA, duration 1.03 sec. (ii) For various temperature of the water, heating current 280 mA, duration 1.30 sec.

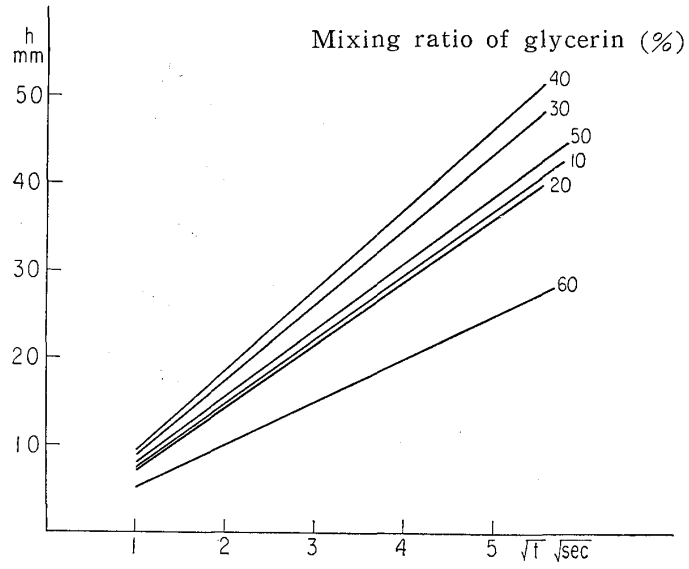

(i)

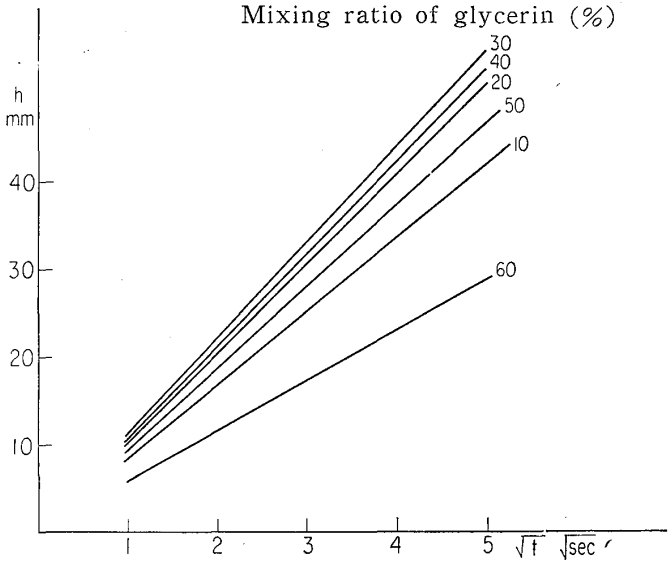

(ii)

Fig. 4 (b). $h \sim \sqrt{t}$ mixture of glycerin and water (20°C). (i) For various mixing ratio, heating current 280 mA, duration 1.03 sec.(ii) For various mixing ratio, heating current 280mA, duration 1.30 sec.

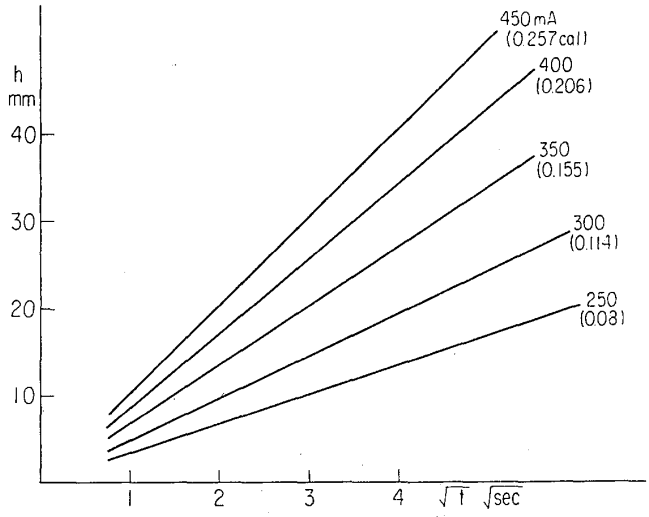

Fig. 5. $h \sim \sqrt{t}$ water (20°C). for various heating current, duration 1.0 sec.

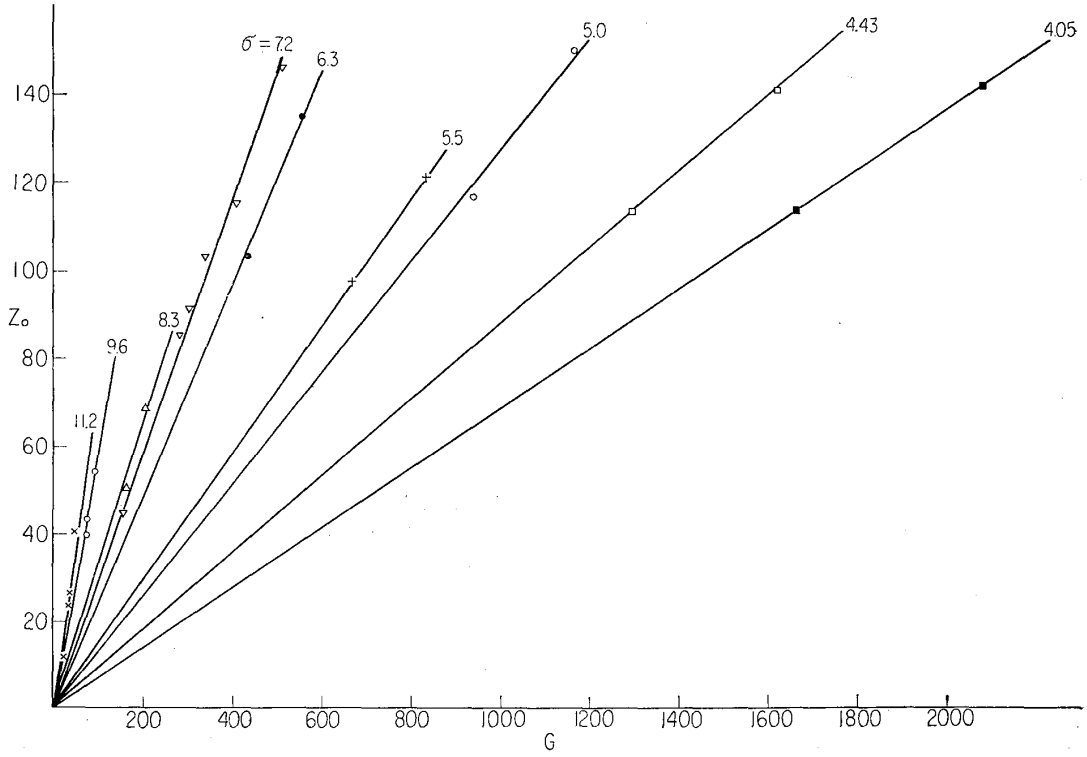

F.ig. 6. (a) $Z_0 \sim G$, water.

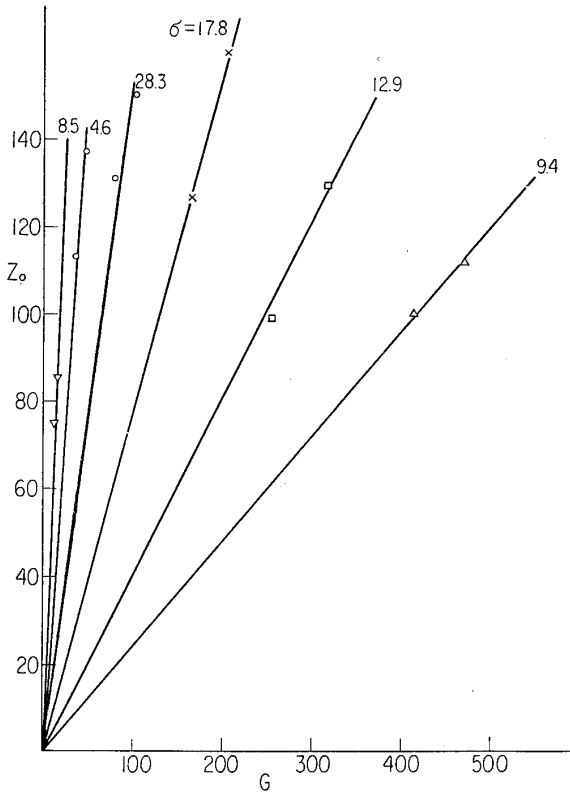

Fig. 6 (b). $Z \sim G$ mixture of glycerin and water.

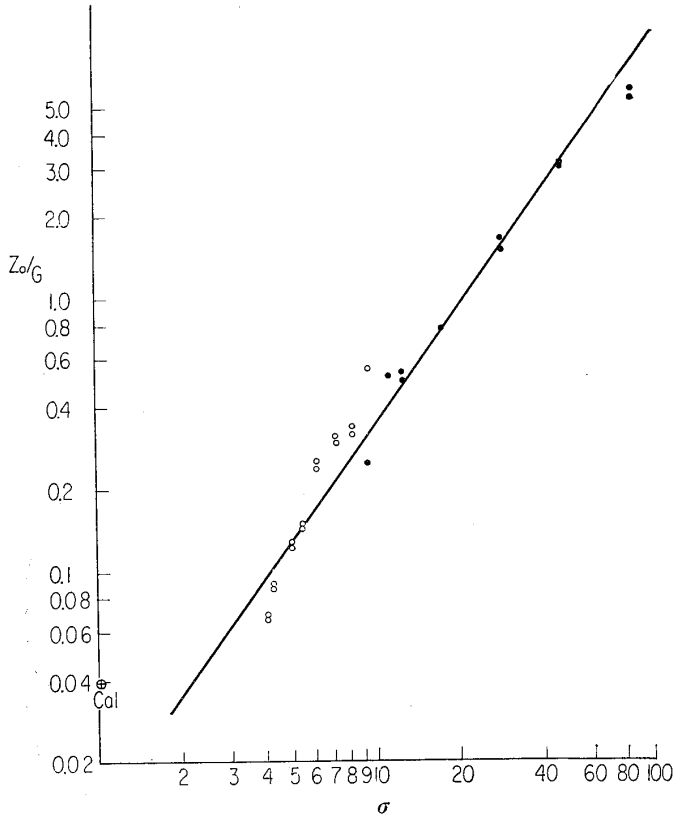

Fig. 7. $Z_0/G \sim \sigma$. ○ water, ● mixture of glycerin and water.

References

1) S. Goldstein (ed): *Modern Developments in Fluid Dynamics*, (Clarendon press, Oxford 1938).
2) H. Schlichting: *Grenzschicht-Theorie* (Verlag G. Braun, Karlsruhe. 1951).
3) L.D. Landau and E.M. Lifshitz: *Fluid Mechanics*, trans. by J.B. Sykes and W.H. Reid (Pergamon Press, London, 1959).
4) B. Woodward: Quat. J.R. Meteor. Sci. **86** (1959) 144.
5) R.S. Scorer: J. Fluid Mech. **2** (1957) 583.
6) B.R. Morton, G.I. Taylor and J.S. Turner: Proc. Roy. Soc. London A **234** (1956) 1.
7) J.S. Turner: Proc. Roy. Soc. London A **239** (1957) 61.
8) J.S. Turner: J. Fluid Mech. **7** (1960) 419.
9) B.R. Morton: J. Fluid Mech. **9** (1960) 107.
10) Sedov: *Similarity* and *Dimensional Analysis* in *Mechanics*, trans. by M. Holt and M. Friedman (Infoserch Ltd. London, 1959).
11) R. Chevalerias, Y. Laton and C. Veret: J. Opt. Soc. Amer. **74** (1957) 703.